ISSN 1063-7761, Journal of Experimental and Theoretical Physics, 2018, Vol. 127, No. 6, pp. 1033–1039. © Pleiades Publishing, Inc., 2018.
Original Russian Text © A.V. Fetisov, S.Kh. Estemirova, V.Ya. Mitrofanov, S.A. Uporov, 2018, published in Zhurnal Eksperimental'noi i Teoreticheskoi Fiziki, 2018, Vol. 154, No. 6, pp. 1121–1128.

ORDER, DISORDER, AND PHASE TRANSITION IN CONDENSED SYSTEM

Evolution of the Crystal and Electronic Structures of the $RBa_2Cu_3O_{6+\delta}$ Cuprates in Annealing

A. V. Fetisov[a,*], S. Kh. Estemirova[a,b], V. Ya. Mitrofanov[a], and S. A. Uporov[a]

[a] *Institute of Metallurgy, Ural Branch, Russian Academy of Sciences, ul. Amundsena 101, Yekaterinburg, 620016 Russia*
[b] *El'tsin Ural Federal University, ul. Mira 19, Yekaterinburg, 620000 Russia*
**e-mail: fetisovav@mail.ru*

Received April 14, 2018

Abstract—The crystal structure and the magnetic properties of the HTSC cuprates $YBa_2Cu_3O_{6+\delta}$, $Y_{1-x}Ca_xBa_2Cu_3O_{6+\delta}$, and $Nd_{1+x}Ba_{2-x}Cu_3O_{6+\delta}$ ($x = 0.2$) with the structure of a layered perovskite are studied. The well-known aging effect detected in these HTSC materials during storage under standard conditions, namely, an increase in their critical temperature T_c and a decrease in lattice parameter c in time, is investigated. Using $YBa_2Cu_3O_{6+\delta}$ as an example, we show that the dependence of c on the oxygen content undergoes the following changes in time: (1) the negative slope of the dependence with respect to axis δ increases and (2) nonlinearity appears and grows in time according to a quadratic law. The first type of changes is explained by an increase in the valence of copper ions, which is accompanied by a decrease in their radius. The second type is explained by the electrostatic interaction of structural CuO_2 planes due to the accumulation of electron holes, which come from CuO_δ planes, in them. The calculation of the second type of changes in parameter c in the $YBa_2Cu_3O_{6+\delta}$ cuprate exhibits good quantitative agreement with the experimental data. The second-type changes in the $Y_{1-x}Ca_xBa_2Cu_3O_{6+\delta}$ compound (hole doping of CuO_2 planes) turn out to be identical to those in $YBa_2Cu_3O_{6+\delta}$. However, the differently directed (in time) changes in lattice parameter c in $Nd_{1+x}Ba_{2-x}Cu_3O_{6+\delta}$ indicate that the CuO_2 planes in the neodymium cuprate are doped by electrons at the initial stage of aging. However, when these planes are saturated with holes in time, the type of doping changes from n to p without a noticeable change in the crystal structure, which has been considered to be impossible for layered cuprates to date.

DOI: 10.1134/S1063776118120051

1. INTRODUCTION

The authors of [1–3] showed that some properties of quenched $RBa_2Cu_3O_{6+\delta}$ (R = lanthanide or Y), which is a high-temperature superconductor, such as lattice parameter c and superconducting transition temperature T_c, can change substantially during storage at room temperature. For example, T_c increases from zero to 20 K and parameter c decreases by 0.04% upon storage of quenched $YBa_2Cu_3O_{6.41}$ for several days [1]. This aging effect is thought to be related to the ordering of oxygen ions in the CuO_δ basal plane, which is accompanied by the formation of defectless copper–oxygen chains [1–3]. This ordering is considered to increase the hole carrier concentration in both CuO_δ and the neighboring CuO_2 planes and, hence, T_c. However, the existence of a direct relation between the oxygen ordering and the hole charge concentration in $RBa_2Cu_3O_{6+\delta}$ has not been experimentally supported. In addition, the authors of [4] comprehensively analyzed the available data and concluded that the arguments for this relation were untenable. This problem cannot be now solved because of the absence of a reliable method to determine the hole charge concentration in CuO_2 planes (q), which provide high-temperature superconductivity. The existing methods, namely, the calculation of bond valence sums (BVS) for the atoms in CuO_2 planes [5] and the use of an empirical relation between q and thermoelectric power measured at room temperature [6], cannot be considered as reliable due to a number of factors. For example, the measured thermoelectric power is a function of the state of both structural CuO_2 planes and CuO_δ planes, which have metallic conduction. In turn, the BVS calculation method needs a precision structural analysis, which can hardly be achieved in studying, e.g., the initial stage of aging.

In this work, we propose a simple and unique method to determine the type and concentration of free carriers in the structural CuO_2 planes in layered $RBa_2Cu_3O_{6+\delta}$ cuprates by analyzing the nonlinear shape of experimental $c(\delta)$ dependences. Using this method, we have shown that the oxygen orderings that occur in $RBa_2Cu_3O_{6+\delta}$ at various δ do not lead to

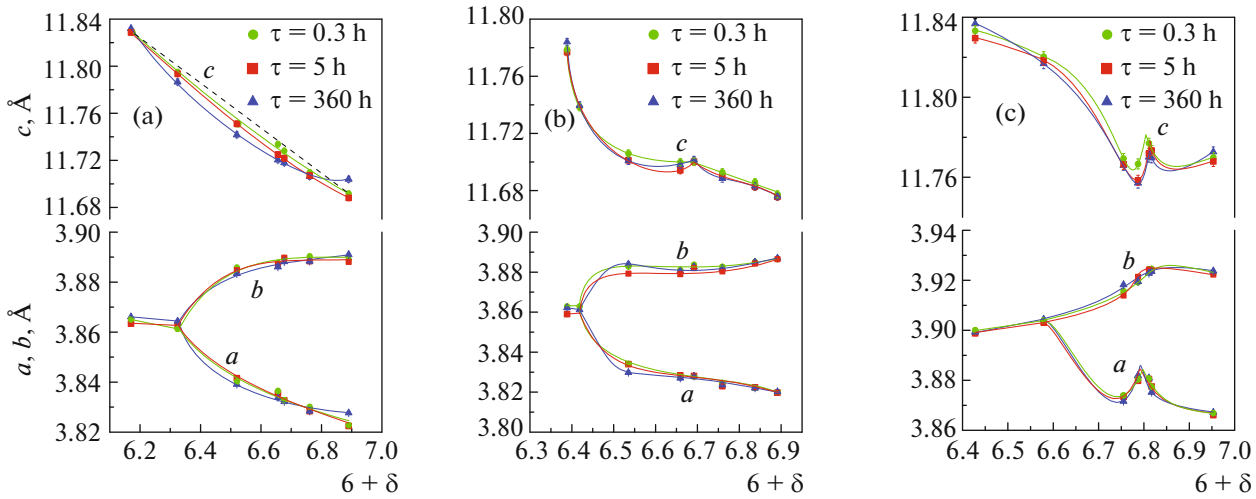

Fig. 1. (Color online) Experimental dependences of lattice parameters a, b, and c on the oxygen content and time τ elapsed after quenching from the oxidation annealing temperature for (a) $YBa_2Cu_3O_{6+\delta}$, (b) $Y_{0.8}Ca_{0.2}Ba_2Cu_3O_{6+\delta}$, and (c) $Nd_{1.2}Ba_{1.8}Cu_3O_{6+\delta}$.

noticeable changes in q, which supports Tallon's statement [5]. We also have found that heterovalent substitution at the cation sites next to a structural CuO_2 plane results in the following effect, which is similar to the well-known 1/8 anomaly [7–9]: a sharp drop in T_c in the narrow δ range that corresponds to a hole concentration of 1/8 in a CuO_2 plane. In this work, we use some results from our earlier works [10, 11].

2. EXPERIMENTAL

Cuprates $YBa_2Cu_3O_{6+\delta}$, $Y_{1-x}Ca_xBa_2Cu_3O_{6+\delta}$, and $Nd_{1+x}Ba_{2-x}Cu_3O_{6+\delta}$ ($x = 0.2$) were synthesized using oxides Y_2O_3, Nd_2O_3, and CuO and barium carbonate at $T = 950$°C for 100 h (R = Y) and $T = 1000$°C for 48 h (R = Nd). The synthesized products contained at most 0.5% impurity phases. To synthesize samples with various oxygen contents, we performed additional oxidation annealing at various temperatures from the range 470–940°C in air and subsequent quenching. The oxygen content was determined from the change in the sample mass after additional oxidation in air at $T = 470$°C for 1 h on the assumption that this procedure results in an oxygen content $(6 + \delta)$ of 6.90 (R = Y) and 6.95 (R = Nd) [12, 13].

Samples with various oxygen contents after various times elapsed after quenching (τ) were studied by X-ray diffraction (XRD) on a 7000 Shimadzu diffractometer. An X-ray diffraction pattern was recorded in 30 min, and the center of this time interval was taken to calculate τ. Each sample was analyzed three times, at $\tau = 0.3$, 5, and 360 h. The unit cell parameters were determined by the least squares method using 14 diffraction lines recorded in the angular range $2\Theta = 20°$–$70°$. The root-mean-square deviation between the calculated and measured line positions was $\overline{\Delta 2\Theta} = 0.015°$. Magnetic measurements were carried out on a Cryogenic CFS-9T-CVTI vibrating-sample magnetometer under field cooling (FC) conditions in a field of 50 Oe. The samples were cooled and heated at a rate of 1 K min^{-1}.

3. EXPERIMENTAL RESULTS

Figure 1 shows the experimental dependences of the lattice parameters on the oxygen content obtained various time intervals after quenching of samples of various compositions. The curves of a and b reflect the tetragonal–orthorhombic phase transition at an oxygen content of 6.33 for $YBa_2Cu_3O_{6+\delta}$, 6.42 for $Y_{0.8}Ca_{0.2}Ba_2Cu_3O_{6+\delta}$, and 6.59 for $Nd_{1.2}Ba_{1.8}Cu_3O_{6+\delta}$. The $c(\delta)$ dependence for the $YBa_2Cu_3O_{6+\delta}$ samples is linear at $\tau \to 0$ and changes into a nonlinear dependence with a gradual increase in a nonlinear contribution when storage time τ increases. The $c(\delta)$ dependences for heterovalent substitution samples are nonlinear even at $\tau \to 0$ and have a singularity near $(6 + \delta) = 6.7$ for $Y_{0.8}Ca_{0.2}Ba_2Cu_3O_{6+\delta}$ and 6.8 for $Nd_{1.2}Ba_{1.8}Cu_3O_{6+\delta}$ for all storage times.

Figure 2 shows the results of low-temperature magnetic measurements of the samples after aging for 360 h. It should be noted that this storage time after quenching serves as the approximation $\tau \to \infty$, since parameters c and T_c were found to remain unchanged further. The $T_c(\delta)$ dependences found for the samples under study are seen to be either steplike curves with two plateaus at $T = 55$ and 90 K for $YBa_2Cu_3O_{6+\delta}$ or fragments of steplike curves, which is most pronounced for the $Nd_{1.2}Ba_{1.8}Cu_3O_{6+\delta}$ cuprate (Fig. 2f; experimental curve, extrapolating dashed line). The $T_c(\delta)$ dependences obtained for unsubstituted $YBa_2Cu_3O_{6+\delta}$ [14] and $NdBa_2Cu_3O_{6+\delta}$ [15]

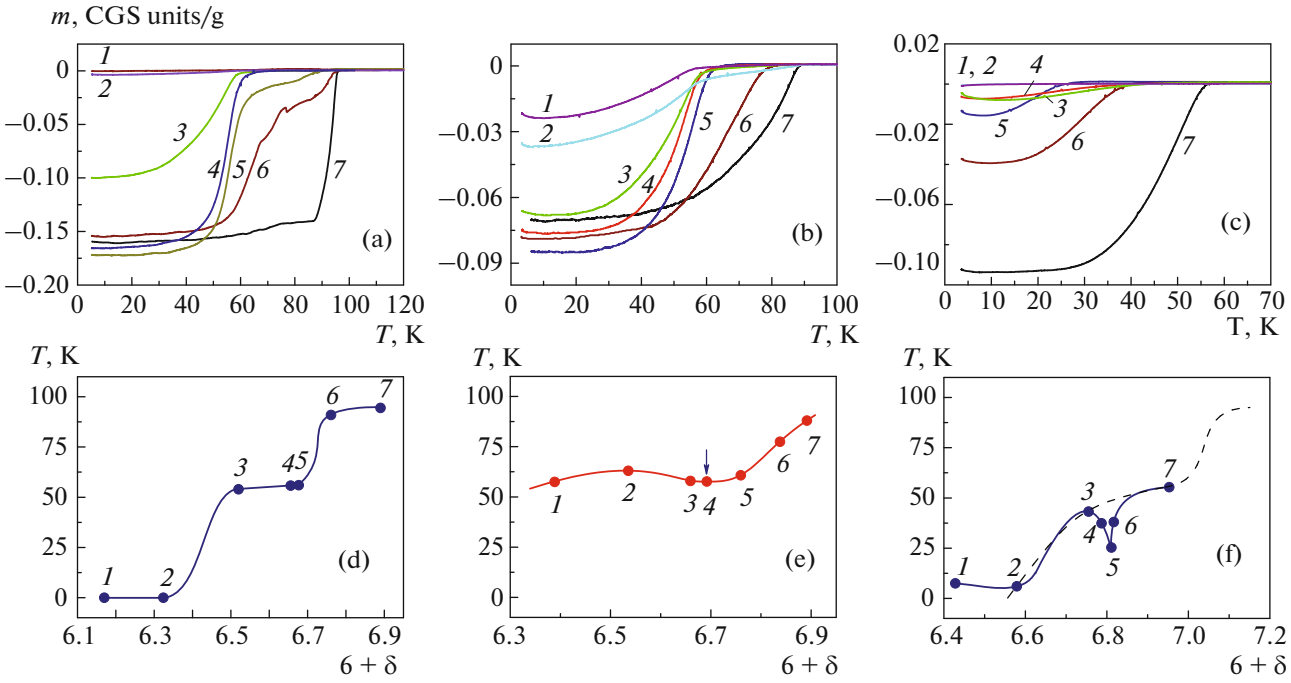

Fig. 2. (Color online) (a–c) Temperature dependences of magnetization and (d–f) T_c^{onset} (onset of superconducting transition) vs. the oxygen content determined from the magnetization curves: (a, d) $YBa_2Cu_3O_{6+\delta}$, (b, e) $Y_{0.8}Ca_{0.2}Ba_2Cu_3O_{6+\delta}$, and (c, f) $Nd_{1.2}Ba_{1.8}Cu_3O_{6+\delta}$. The arrow indicates a drop in T_c in the vicinity of $\delta = 0.7$ for $Y_{0.8}Ca_{0.2}Ba_2Cu_3O_{6+\delta}$.

are similar to the curve in Fig. 2d and the dashed line in Fig. 2f. Thus, heterovalent substitution in the cuprates under study leads to the shift of the $T_c(\delta)$ dependences toward high δ if Ca substitutes for Y and toward low δ when Nd substitutes for Ba.

It is also seen in Fig. 2 that the critical temperature decreases in the vicinity of the compositions $(6 + \delta) = 6.7$ for $Y_{1-x}Ca_xBa_2Cu_3O_{6+\delta}$ and 6.8 for $Nd_{1+x}Ba_{2-x}Cu_3O_{6+\delta}$. This δ range coincides with the corresponding range of increasing lattice parameter c (and also parameter a for the neodymium composition).

4. DISCUSSION OF RESULTS

The observed local decrease in the critical temperature of the substituted cuprates at certain values of δ resembles the suppression of T_c in some HTSC cuprates at a free carrier concentration of 1/8 (e.g., T_c of $La_{2-x}Sr_xCuO_4$ decreases by 20 K at $x = 0.21$ [7]) [7–9]. At this average charge concentration, so-called stripes, i.e., static charge ordering in the form of alternating high- and low-charge-density regions, appear. In this case, integral T_c of a material is specified by the areas that have the worst superconducting characteristics (i.e., low-charge-density regions). Although no local decrease in T_c of $RBa_2Cu_3O_{6+\delta}$ has been detected at any values of δ, the authors of [16] think that these compounds are thermodynamically close to the state of statically charges stripes. At least, they have dynamic stripe correlations, which could become static in the presence of sufficiently effective pinning centers [9, 17]. The charge heterogeneity that is formed at the sites adjacent to a CuO_2 plane in $RBa_2Cu_3O_{6+\delta}$ during heterovalent substitution is thought to be translated to this plane and to initiate the appearance of charge stripes at a certain value of δ.

We now dwell on the dependences of lattice parameter c on δ obtained for the unsubstituted $YBa_2Cu_3O_{6+\delta}$ cuprate (Fig. 1a). The following feature is clear: the nonlinearity of the curves increases with the time elapsed after quenching. The symbols in Fig. 3 indicate the extracted nonlinear part of the experimental $c(\delta)$ dependences for the $YBa_2Cu_3O_{6+\delta}$ composition. Our main assumption is that the dependences shown in Fig. 3 reflect the hole charge transfer from the structural CuO_δ plane to CuO_2 plane, which takes place during both the oxygen saturation of $YBa_2Cu_3O_{6+\delta}$ and its natural aging. To prove this assumption, we calculate the nonlinear part $\Delta c^*/c$ of the $c(\delta)$ dependences using the electrostatic equation for interacting charged planes (Fig. 4). In general form, the forces (per unit area) that appear during the charge transfer between the structural CuO_δ planes and CuO_2 can be written as

$$F_1 = \sum_n B_n \frac{(q \cdot p_n)\bar{e}^2}{2\varepsilon_0 \varepsilon^n \sigma^2} + \frac{\bar{e}^2}{2\varepsilon_0 \sigma^2}\left[\frac{(1-2q)q}{\varepsilon^{III}} + \frac{q^2}{\varepsilon^{II}}\right], \quad (1a)$$

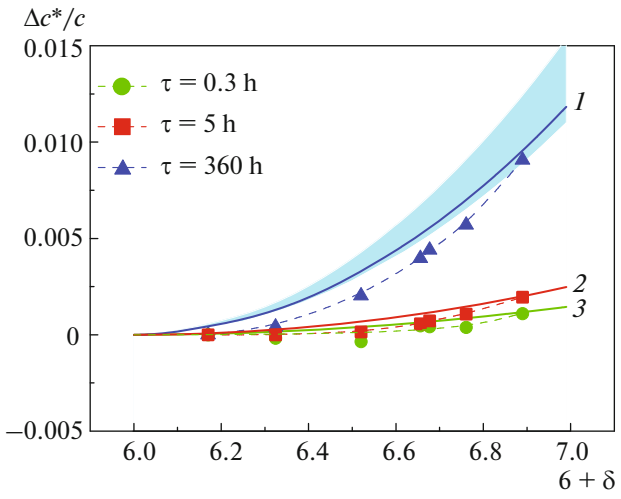

Fig. 3. (Color online) Extracted linear part of the experimental $c(\delta)$ dependences for $YBa_2Cu_3O_{6+\delta}$ (points, dashed lines) Experimental data and (solid lines) calculation by Eqs. (2) and (3). Coloring indicates the range of uncertainty for the curve calculated at $\tau = 360$ h.

$$F_2 = \sum_m B_m \frac{(q \cdot p_m)\bar{e}^2}{2\varepsilon_0 \varepsilon^m \sigma^2} + \frac{q^2\bar{e}^2}{2\varepsilon_0 \varepsilon^{\mathrm{I}} \sigma^2}, \qquad (1b)$$

where p_n and p_m are the specific charge that is likely to exist in the structural planes other than CuO_δ and CuO_2 (here, the effects of these planes exerted on the CuO_2 plane are summed), ε_0 is the permittivity of vacuum, and ε^n and ε^m are the permittivity of the substance confined between the two structural planes under study. For clarity, the three types of spatial regions between CuO_δ and two CuO_2 planes in Fig. 4 are enclosed and designated as I, II, and III. These regions have permittivities ε^{I}, $\varepsilon^{\mathrm{II}}$, and $\varepsilon^{\mathrm{III}}$, and σ is the elementary area in the basal plane ($\sigma = ab$) to which the specific charges q, p_n, and p_m relate. Charge q is related to the oxygen concentration in $YBa_2Cu_3O_{6+\delta}$ by the equation $q \approx 0.187\delta$, which was derived by the BVS method [6]. The quadratic term in Eqs. (1a) and (1b) describes the charge-transfer-induced interaction between the CuO_δ and CuO_2 planes, and the linear terms of these equations describe the interactions of these planes with all other structural elements of the unit cell that contain a nonzero δ-independent charge (e.g., some structural planes should have a total specific charge of -1 to compensate for a charge of $+1$ in CuO_δ; see Fig. 4). To achieve our purposes, we only consider the nonlinear terms in Eqs. (1a) and (1b),

$$F_1' = \frac{q^2\bar{e}^2}{2\varepsilon_0 \varepsilon^{\mathrm{II}} \sigma^2} - \frac{2q^2\bar{e}^2}{2\varepsilon_0 \sigma^2 \varepsilon^{\mathrm{III}}}, \qquad (2a)$$

$$F_2' = \frac{q^2\bar{e}^2}{2\varepsilon_0 \varepsilon^{\mathrm{I}} \sigma^2}. \qquad (2b)$$

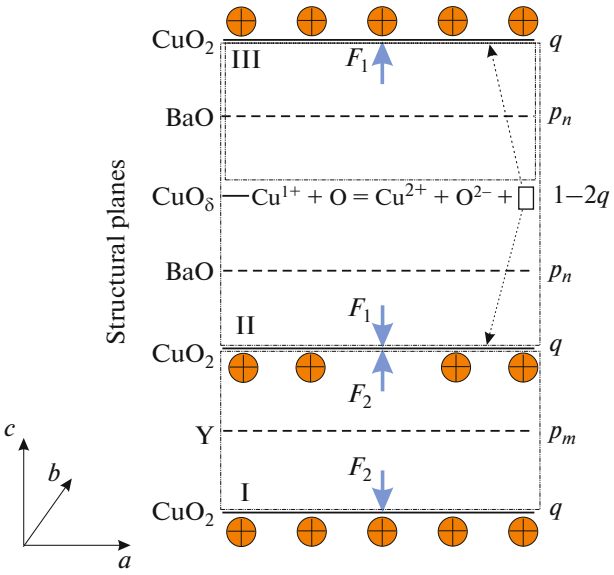

Fig. 4. (Color online) Electrostatic forces F_1 and F_2 on the structural CuO_2 planes within the unit cell of $YBa_2Cu_3O_{6+\delta}$. The charges localized at the structural planes are indicated to the right of them. The reaction of hole formation in the CuO_δ plane is presented.

The relative change in lattice parameter c caused by the electrostatic interaction of the structural planes is

$$\frac{\Delta c}{c} = \frac{2F_1'/3 + F_2'/3}{\varepsilon_{33}}, \qquad (3)$$

where ε_{33} is the elastic modulus of the lattice along direction c. Substituting the values $\varepsilon_0 = 8.854 \times 10^{-12}$ C/(n m^2), $\varepsilon^{\mathrm{I}} = \varepsilon^{\mathrm{II}} = 1$, $\varepsilon^{\mathrm{III}} = 4$, $\sigma^2 = 1.5 \times 10^{-38}$ m^4, $\varepsilon_{33} = 186$ GPa [19], and $q = 0.187\delta$ into Eqs. (2) and (3), we find dependence $\Delta c/c$, which well describes the experimental curve for the case $\tau = 360$ h (Fig. 3, curve *1*).[1,2,3] The coloring in Fig. 3 indicates the error range for the calculated $\Delta c/c$ curve that is related to the uncertain value of $\varepsilon^{\mathrm{III}}$ and the possible difference

[1] The value taken for ε^{I} and $\varepsilon^{\mathrm{II}}$ is explained by the fact that, according to the electrostatics laws, the electric field that is induced by the charges in CuO_2 planes inside closed contours I and II indicated by the dot-and-dash line in Fig. 4 is zero. Therefore, the substance should not react to the appearance of charges in CuO_2.

[2] On the other hand, Ba^{2+}–O^{2-} ionic layers are located between CuO_2 and CuO_δ planes (inside contour III), and these layers are easily polarized by the field of these planes [18]. Then, parameter $\varepsilon^{\mathrm{III}}$ can be estimated as the permittivity characteristic of ionic compounds ($\varepsilon = 4$–10). It should be noted that parameter ε in this range weakly affects the resulting value of $\Delta c/c$. The calculation showed that, when ε increased in this range, $\Delta c/c$ increased only by 30%.

[3] According to [20, 21], we can assume that the structural unit inside contour II (see Fig. 4) has a higher hardness than the unit inside contour I (hereafter, structural units II and I). This difference cannot be taken into account without certain data. Nevertheless, if we consider the limiting case and assume that the elastic modulus of unit I is ∞ (then, the elastic modulus of unit II should be two-thirds of the integrated experimental value of ε_{33}), we can readily show that $\Delta c/c$ decreases only by 7%.

between the elastic moduli of structural units I and II (see Fig. 4). The good quantitative agreement between the calculated curve and the experimental data allows us to think that our main assumption is correct. Then, the experimental curves obtained at $\tau = 0.3$ h and 5 h in Fig. 3 reflect the situation where the charge transfer from the CuO_δ plane to the CuO_2 plane is incomplete. These curves are described by the equations given above, where charge q is multiplied by 0.32 or 0.48 for $\tau = 0.3$ or 5 h, respectively (Fig. 3; curves *3*, *2*).

Thus, we found that the nonlinear $c(\delta)$ dependences of the $YBa_2Cu_3O_{6+\delta}$ cuprate is directly related to the free carrier (hole) concentration in its structural CuO_2 planes and that the extracted nonlinear part of these dependences is proportional to the charge concentration squared. Based on this thesis, we try to analyze the $c(\delta)$ dependences obtained for the substituted $RBa_2Cu_3O_{6+\delta}$ cuprates (see Figs. 1b, 1c). These dependences are substantially nonlinear in the as-quenched state, and an analysis of the causes of this behavior is beyond the scope of this work. This initial nonlinearity can be not related to the charge accumulated on CuO_2 planes. Nevertheless, below we will show that useful information can be obtained from these dependences. Here, we analyze the changes in them that occur in time after quenching rather than the dependences themselves. The nonlinear part is extracted from the $\Delta c/c$ differential dependences on the assumption that this nonlinearity is associated with the electrostatic interaction of CuO_2 planes.

Figure 5 shows the $\Delta c/c$ differential dependences obtained by the subtraction of $c(\delta)|_{\tau = 0.3}$ from the curves corresponding to $\tau = 5$ and 360 h and by division by parameter c. Figure 6 depicts the separated nonlinear parts $\Delta c^*/c$ of these differential dependences. We now qualitatively analyze these nonlinear parts. For the $Y_{1-x}Ca_xBa_2Cu_3O_{6+\delta}$ cuprate, the nonlinearity of the $\Delta c^*/c(\delta)$ curve increases with time, which is similar to the behavior of the unsubstituted yttrium–barium cuprate (see Fig. 6a). The heterovalent substitution in $Y_{1-x}Ca_xBa_2Cu_3O_{6+\delta}$ implies the doping of its CuO_2 planes by electron holes without a charge redistribution between the planes (i.e., the CuO_2 planes are not positively charged upon this doping), and no other differences from the electronic structure of $YBa_2Cu_3O_{6+\delta}$ are observed here [6, 22]. Therefore, the change $\Delta c^*/c(\delta)$ in time is to be identical to that in unsubstituted $YBa_2Cu_3O_{6+\delta}$. However, the $\Delta c^*/c(\delta)$ dependence obtained for $Nd_{1+x}Ba_{2-x}Cu_3O_{6+\delta}$ changes in time differently (see Fig. 6b). The $\Delta c^*/c(\delta)$ curve bends toward negative values of $\Delta c^*/c$ at the initial stage and only later acquires conventional positive dynamics. This behavior obviously follows from the assumption that, upon the substitution of Nd^{3+} for Ba^{2+}, the CuO_2 planes are doped with electrons and the charge is redistributed between the BaO and CuO_2 planes (see Fig. 4). This implies initial repulsion of the

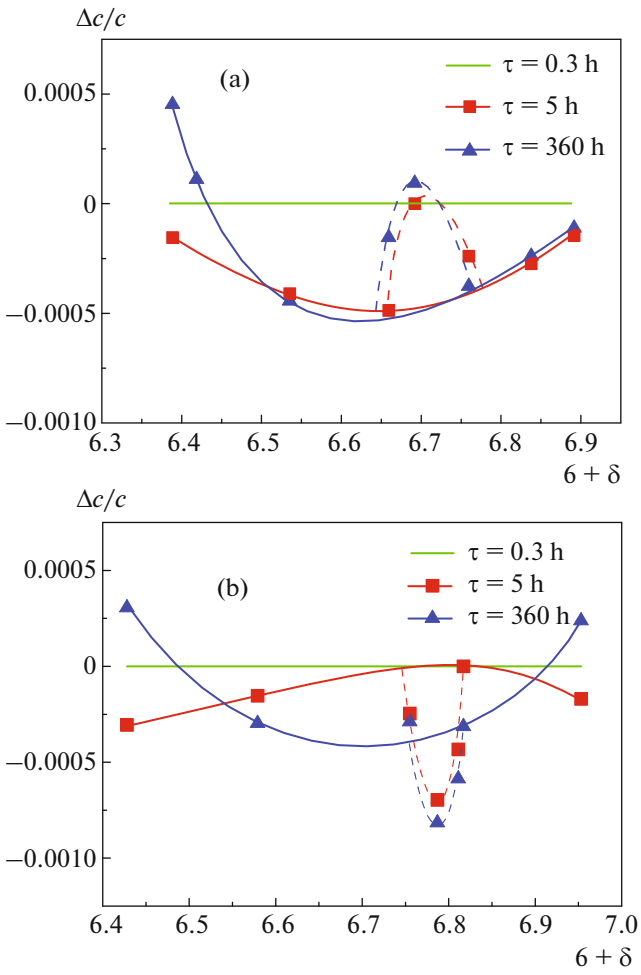

Fig. 5. (Color online) Relative changes in lattice parameter c corresponding to aging times of 5 and 360 h that were obtained from the $c(\delta)$ dependences for (a) $Y_{0.8}Ca_{0.2}Ba_2Cu_3O_{6+\delta}$ and (b) $Nd_{1.2}Ba_{1.8}Cu_3O_{6+\delta}$. These changes were determined by the subtraction of the experimental data obtained at a holding time $\tau = 0.3$ h.

structural CuO_2 planes because of the negative charge localized on them. However, when electron holes come to these planes, the modulus of the total charge on these planes first decreases in time and then increases after the recombination of all electrons with electron holes.

However, we encounter the problem associated with the following well-known empirical rule related to a change in the type of carrier in the electronic system of layered cuprates: this change cannot occur without substantial lattice restructuring [23]. This rule is based on unsuccessful attempts to synthesize a layered n-type conduction cuprate with CuO_2 layers. Based on these data, the generally accepted point is that the excess electron caused by the substitution of Nd for Ba forms a bond with oxygen, which is additionally supplied from outside and is localized in CuO_δ planes, rather than doping CuO_2 planes. Indeed, the

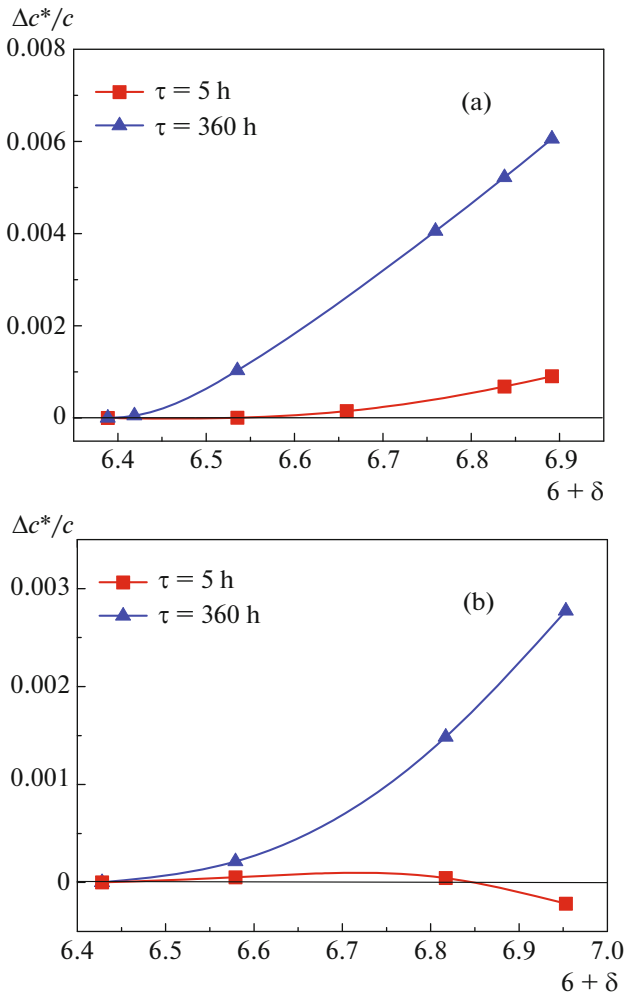

Fig. 6. (Color online) Extracted linear parts of the $\Delta c/c(\delta)$ dependences for $\tau = 5$ and 360 h obtained for (a) $Y_{0.8}Ca_{0.2}Ba_2Cu_3O_{6+\delta}$ and (b) $Nd_{1.2}Ba_{1.8}Cu_3O_{6+\delta}$.

equilibrium oxygen content in $Nd_{1+x}Ba_{2-x}Cu_3O_{6+\delta}$ exceeds that in $Nd_2Ba_2Cu_3O_{6+\delta}$ according to various data. However, an exception from this rule has recently been detected [24]: the type of conduction in $Y_{0.38}La_{0.62}(Ba_{0.87}La_{0.13})Cu_3O_y$ changed from *n* to *p* without a noticeable change in the crystal structure during the oxygen saturation of the solid solution. This solid solution is a close analog of our substituted neodymium cuprate. According to our qualitative analysis, the heterovalent substitution in $Nd_{1+x}Ba_{2-x}Cu_3O_{6+\delta}$ at least partly causes electron doping of the system, and the type of carrier is gradually changed as the cuprate is saturated with oxygen. Thus, this compound is likely to be another exception from the empirical rule proposed in [23].

Note that the experimental $\Delta c^*/c(\delta)$ curves in Fig. 3 have no singularities (inflection points) at the values of δ corresponding to the structural transitions in $YBa_2Cu_3O_{6+\delta}$, namely, tetra → ortho-II ($\delta = 0.32$), ortho-II → ortho-III ($\delta = 0.63$), ortho-III– ortho-I ($\delta = 0.77$), and so on [25–27]. This means that the oxygen ordering in this compound does not affect the carrier concentration in CuO_2. Therefore, the assumption [1–3] that the aging effect in $RBa_2Cu_3O_{6+\delta}$ is related to the oxygen ordering that occur at room temperature is likely to be erroneous. The aging of these cuprate superconductors is thought to be related to the kinetic difficulties of the charge transfer from CuO_δ to CuO_2 planes, which proceeds according to the relatively long chain $O_{CuO_\delta} \rightarrow Cu_{CuO_\delta} \rightarrow O_{ap} \rightarrow Cu_{CuO_2} \rightarrow O_{CuO_2}$ (where O_{ap} is apical oxygen connecting CuO_δ to CuO_2 planes).

In addition, our model does not exclude a possible dependence of critical temperature T_c on the oxygen ordering in $RBa_2Cu_3O_{6+\delta}$. However, this dependence can be explained by other factors, such the stresses appearing in CuO_2 planes [28, 29].

5. CONCLUSIONS

(1) The heterovalent substitution of cations near a structural CuO_2 layer at a level of 20% causes an effect, which is similar to the 1/8 anomaly and is represented by a dip in the $T_c(\delta)$ dependence near a concentration $q = 1/8$.

(2) Based on an analysis of the $c(\delta)$ dependences, we proposed a new method to determine the charge concentration in the structural CuO_2 planes of $RBa_2Cu_3O_{6+\delta}$ cuprates.

ACKNOWLEDGMENTS

This work was carried out in terms of state assignment no. 0396-2015-0075 using the equipment of the Center for Collective Use Ural-M of the Institute of Metallurgy.

REFERENCES

1. J. D. Jorgensen, S. Pei, P. Lightfoot, et al., Phys. C **167**, 571 (1990).
2. J. Kircher, M. Cardona, A. Zibold, et al., Phys. Rev. B **48**, 9684 (1993).
3. A. Knizhnik, G. M. Reisner, O. Shafir, et al., Supercond. Sci. Technol. **17**, 448 (2004).
4. R. McCormack, D. de Fontaine, and G. Ceder, Phys. Rev. B **45**, 12976 (1992).
5. J. L. Tallon, Phys. C (Amsterdam, Neth.) **176**, 547 (1991).
6. J. L. Tallon, C. Bernhard, H. Shaked, et al., Phys. Rev. B **51**, 12911 (1995).
7. A. R. Moodenbaugh, Youwen Xu, and M. Suenaga, Phys. Rev. B **38**, 4596 (1988).
8. K. Kawamura, Y. Kobayashi, C. Kobashi, et al., J. Supercond. Nov. Magn. **30**, 2037 (2017).

9. Y. Koike, M. Akoshima, M. Aoyama, et al., Phys. C (Amsterdam, Neth.) **357–360**, 82 (2001).
10. A. V. Fetisov, G. A. Kozhina, S. Kh. Estemirova, et al., Phys. C (Amsterdam, Neth.) **515**, 54 (2015).
11. A. V. Fetisov and S. Kh. Estemirova, J. Supercond. Nov. Magn. **31**, 203 (2018).
12. E. D. Specht, C. J. Sparks, A. G. Dhere, et al., Phys. Rev. B **37**, 7426 (1988).
13. T. B. Lindemer, E. D. Specht, P. M. Martin, et al., Phys. C **255**, 65 (1995).
14. R. J. Cava, B. Batlogg, K. M. Rabe, et al., Phys. C **156**, 523 (1988).
15. B. W. Veal, J. Jr. Faber, R. L. Hitterman, et al., Phys. Rev. B **41**, 4173 (1990).
16. S. Sanna, P. Manca, S. Agrestini, et al., Int. J. Mod. Phys. B **14**, 3668 (2000).
17. M. Arai, T. Nishijima, Y. Endoh, et al., Phys. Rev. Lett. **83**, 608 (1999).
18. S. Sh. Shil'shtein and A. S. Ivanov, Phys. Solid State **37**, 1796 (1995).
19. M. Lei, J. L. Sarrao, W. M. Visscher, et al., Phys. Rev. B **47**, 6154 (1993).
20. H. Zhang, Phys. C (Amsterdam, Neth.) 364–365, 151 (2001).
21. R. J. Cava, A. W. Hewat, E. A. Hewat, et al., Phys. C (Amsterdam, Neth.) **165**, 419 (1990).
22. E. F. Talantsev, N. M. Strickland, S. C. Wimbush, et al., Appl. Phys. Lett. **104**, 242601 (2014).
23. Y. Tokura and T. Arima, Jpn. J. Appl. Phys. **29**, 2388 (1990).
24. K. Segawa and Y. Ando, Phys. Rev. B **74**, 100508 (2006).
25. R. Liang, D. A. Bonn, and W. N. Hardy, Phys. C **336**, 57 (2000).
26. G. Calestani, P. Manca, S. Sanna, et al., Int. J. Mod. Phys. B **13**, 1073 (1999).
27. M. V. Zimmermann, J. R. Schneider, T. Frello, et al., Phys. Rev. B **68**, 104515 (2003).
28. S. Agrestini, N. L. Saini, G. Bianconi, and A. Bianconi, J. Phys. A: Math. Gen. **36**, 9133 (2003).
29. A. Bianconi, G. Bianconi, S. Caprara, et al., J. Phys.: Condens. Matter **12**, 10655 (2000).

Translated by K. Shakhlevich